Relic Crystal-Lattice Effects on Raman Compression of Powerful X-Ray Pulses in Plasmas

V. M. Malkin and N. J. Fisch

Department of Astrophysical Sciences, Princeton University, Princeton, New Jersey 08544, USA

(Received 8 May 2007; published 12 November 2007)

Powerful x-ray pulses might be compressed to even greater powers by means of backward Raman amplification in ultradense plasmas produced by ionizing condensed matter by the same pulses. The pulse durations contemplated are shorter than the time for complete smoothing of the crystal lattice by thermal motion of ions. Although inhomogeneities are generally thought to be deleterious to the Raman amplification, the relic lattice might, in fact, be useful for the Raman amplification. The x-ray frequency band gaps can suppress parasitic Raman scattering of amplified pulses, while enhanced dispersion of the x-ray group velocity near the gaps can delay self-phase-modulation instability, thereby enabling further amplification of the x rays.

DOI: 10.1103/PhysRevLett.99.205001 PACS numbers: 52.38.−r, 41.60.Cr, 42.55.Vc, 42.65.Re

New mJ x-ray laser technologies [1–3] might produce attosecond laser pulses of intensities (power densities) comparable to the laser intensities currently pursued by the MJ optical laser technologies [4,5]. The currently projected durations of powerful x-ray pulses are of the order of 100 fs. There are proposals to reduce the output pulse to durations somewhat shorter than a femtosecond, though in the process much reducing the pulse energy [6].

Efficient compression of powerful x-ray pulses to even shorter durations might be accomplished by means of backward Raman amplification (BRA) in plasmas, as proposed in [7]. This proposal relied on highly uniform plasmas. However, plasmas produced by the sudden ionization of crystals may be less uniform, because thermal ion motion would not smooth the ion lattice within the ultrashort x-ray pulse durations. For instance, for a 0.3 fs pulse, the ion temperature needed for the lattice smoothing would be about A keV, where A is the atomic weight of ions ($A = 1$ for hydrogen). Such ion temperatures are not readily achievable, since it is the electron plasma that is primarily heated by the x-ray pulses, and the energy exchange between electrons and ions is relatively slow. Neither does the longer-scale electric field produced from the ponderomotive evacuation of the electrons smooth (rather than just deform) the lattice, and a pulse of 0.3 fs duration is 1000 Å long.

As long as the ion lattice survives in some form, the electron concentration follows the lattice patterns, and the respective modulation of the x-ray refraction index will affect x-ray propagation and interactions. This Letter shows that rather than to try to smooth out the relic lattice structure one might exploit it.

To see the possible effects of the relic crystal lattice on x-ray BRA, consider an ideal lattice giving rise to a periodically modulated plasma. The major differences between uniform and periodically modulated plasmas are associated with x-ray frequency band gaps, caused by Bragg scattering, and enhanced dispersion of the x-ray group velocity near the bands. The dispersion might, in fact, be used to manipulate short laser pulses, like Bragg gratings can be used in optical fibers (see, say, [8] and related references). We show that this enhanced dispersion may increase the Raman pulse amplification by delaying the development of the self-phase modulation instability (SPMI), which limits the BRA [9]. The pulse is stretched during the dispersion-dominated stage. It could be recompressed by means of a complementary lattice, similar to how this is accomplished for optical pulses in chirped pulse amplifiers (CPA) [10]. The ballistic pulse recompression occurs as an explosive process (in contrast to the slowing-down BRA), and so can outrun the SPMI.

A further way to exploit the relic lattice is to use the associated x-ray frequency band gap for suppressing the parasitic Raman scattering of the amplified pulses, which also limits the BRA [9]. The typical near-gap dispersion law is shown in Fig. 1. For the gap center downshifted from the amplified pulse by the plasma frequency ω_p, the Stokes components of the pulse get into the gap and cannot propagate in such a system. The suppression of the near-forward Stokes generation increases the allowed amplification distance. The suppression of the backward Stokes generation allows longer pulses of the same intensity. For thin enough pulses, plasma channels might guide the laser pulse and thus avoid side scattering.

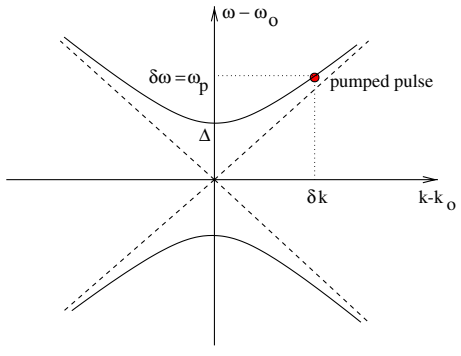

FIG. 1 (color online). The typical near-gap dispersion law. For the gap center downshifted from the pumped pulse by the plasma frequency ω_p, generation of Stokes components is suppressed.

To see quantitatively what advantages might thus accrue due to the relic lattice, consider equations for backward Raman (or Brillouin) amplification, taking into account the dispersion of the group velocity and the nonlinear propagation effects of the amplified pulse:

$$a_t + c_a a_z = V_3 f b, \qquad f_t = -V_3 a b^*, \tag{1}$$

$$b_t - c_b b_z = -V_3 a f^* - \imath c_b' b_{tt}/2c_b + i\imath R|b|^2 b. \tag{2}$$

Here a, b, and f are envelopes of long pump pulse, counterpropagating short pumped pulse, and material wave, respectively; subscripts t and z signify time and space derivatives; c_a and c_b are group velocities of pump and pumped pulse (the material wave group velocity is zero in appropriate reference frame); c_b' is the derivative of the pumped pulse group velocity over the frequency; V_3 is the 3-wave coupling constant (real for appropriately defined wave envelopes); and R is the nonlinear frequency shift constant (due to the Kerr or relativistic electron nonlinearity). The dispersion and self-nonlinearity are taken into account only for the pumped pulse (which is shorter and grows to intensities greater than that of pump). The encountered fresh material waves do not have enough time to exhibit dispersive effects associated with the relic crystal structure within the short pumped pulse duration.

For transient BRA of x rays in plasma, a and b represent space-time envelopes of the vector potentials of the pump and pumped pulse, respectively, in units of $m_e c^2/e \approx 5 * 10^5$ V, $f\sqrt{\omega/2\omega_p}$ is the electrostatic field of the Langmuir wave in units of $m_e c\omega_p/e = c\sqrt{4\pi m_e n_e} \approx \sqrt{n_e[\mathrm{cm}^{-3}]}\mathrm{V/cm}$, $\omega_a \approx \omega_b = \omega \gg \omega_p$, $\omega_a - \omega_b = \omega_p$ (here ω_p is the true resonant plasma eigenmode frequency), $c_a \approx c_b \approx c$, $V_3 = \sqrt{\omega\omega_p/2}$, $R = \omega_p^2/4\omega$ [11]. The pumped pulse duration is larger than ω_p^{-1}, but shorter than the time for plasma ions to be moved. The near-gap dispersion law is $\delta\omega^2 = \Delta^2 + \delta k^2 c_o^2$, where $c_o = d\omega_o/dk_o \approx c$ ($\omega_o^2 = k_o^2 c^2 + \omega_p^2$). For $\delta\omega \gg \Delta$, the near-band dispersion law simplifies to $c\delta k \approx \delta\omega - \Delta^2/2\delta\omega$. Then, $c_b \approx c(1 - \Delta^2/2\delta\omega^2)$, and $c_b'/c_b \approx \Delta^2/\delta\omega^3$. For the suppression of parasitic Raman scattering of the pumped pulse, as depicted in Fig. 1, $\delta\omega = \omega_p$ and $c_b'/c_b \approx \Delta^2/\omega_p^3$.

As long as the dispersion and cubic terms in (2) are negligible, the solutions of Eqs. (1) and (2) are well known. At the linear stage of a long pump pulse backscattering instability [12], the maximum of initially short seed-pulse moves with the speed $c_b/2$ and increases exponentially with the growth rate $a_0 V_3$, where a_0 is the nondepleted pump amplitude. The pulse stretches, since the front moves with the speed c_b. This stage ends when the pump depletion becomes appreciable. Then the nonlinear π-pulse regime [13] is established. The pulse maximum, moving with a superluminous velocity, approaches the pulse front, so that the pulse contracts. The area under the pulse envelope does not change.

As the pulse grows and contracts, its evolution slows down, while the time for dispersion and self-nonlinearity to manifest shortens. When these effects become important, the π-pulse regime ends. Dispersive effects in stimulated 3-wave backscattering were studied previously for regimes where dissipation is important and stationary propagating solitons are relevant [14], which differ from the amplification regimes of interest here. Yet, since the π-pulse duration is much shorter than the pumping time, the quasistatic approximation, $a_t \approx c_b a_z$, is applicable for the pump pulse. Then, basic equations can be reduced to the form

$$\tilde{a}_\zeta = \tilde{b}\tilde{f}, \quad \tilde{f}_\zeta = -\tilde{a}\tilde{b}^*, \quad \tilde{b}_\tau = -\tilde{a}\tilde{f}^* - \imath\tilde{b}_{\zeta\zeta} + \imath Q|\tilde{b}|^2\tilde{b}, \tag{3}$$

with $Q = 2R(c_a + c_b)/V_3^2 c_b'$, by the substitution

$$\zeta = (t + z/c_b)(V_3 a_0)^{2/3}(2c_b/c_b')^{1/3},$$

$$\tau = -z(V_3 a_0/c_b)^{4/3}(c_b'/2)^{1/3}, \qquad f = a_0\sqrt{1 + c_a/c_b}\,\tilde{f},$$

$$a = a_0\tilde{a}, \qquad b = a_0(2c_b a_0^2/c_b' V_3)^{1/3}\sqrt{1 + c_a/c_b}\,\tilde{b}. \tag{4}$$

Remarkably, Q does not depend on the pump amplitude a_0. As seen from Eqs. (3), the dispersion and nonlinearity are of same order in the π-pulse regime, if $|Q| \sim 1$. For $|Q| \gg 1$, the dispersion could not possibly stop SPMI. For $|Q| \ll 1$, the dispersion would prematurely stop the pulse compression much before SPMI could develop. For $|Q| \sim 1$, the dispersion and nonlinearity become important simultaneously at $\tau \sim 1$, precisely as the greatest possible π-pulse compression is reached. Note that for the uniform plasma dispersion, $c_b' \approx c\omega_p^2/\omega^3$, the nonlinearity is stronger than the dispersion, $|Q| = 2c\omega_p/\omega^2|c_b'| \approx 2\omega/\omega_p \gg 1$, so that an enhanced dispersion is really needed to produce an effect before the SPMI develops.

The numerical solution of Eqs. (3) (obtained by complex version of Crank-Nicholson implicit scheme [15]) exhibits, after the π-pulse regime completion, for $|Q| \lesssim 1$, a self-similar pulse stretching at constant intensity. The pulse quanta spread with their relative group velocity, while the pulse intensity remains constant due to the new quanta coming from the pump. The respective self-similar solution (obtained below) appears to be a good approximation to the numerical solution as illustrated by Fig. 2. After pulse stretching a few times, the nonlinear WKB approximation can be used. Taking $\tilde{a} = a_1 e^{i\alpha}$, $\tilde{f} = f_1 e^{i\phi}$, $\tilde{b} = b_1 e^{i\beta}$ with real continuous phases α, ϕ, β and amplitudes a_1, f_1, g_1, one gets from the first two of Eqs. (3) in zero-order WKB approximation:

$$\alpha_\zeta \approx f_1 b_1/a_1, \quad \phi_\zeta \approx a_1 b_1/f_1, \quad \beta + \phi \approx \alpha + \pi/2. \tag{5}$$

A small mismatch between the left and right sides of the last relation enters into the first-order WKB-approximated equations for amplitudes a_1 and f_1. When the phase mismatch is excluded from the amplitude equations, just one

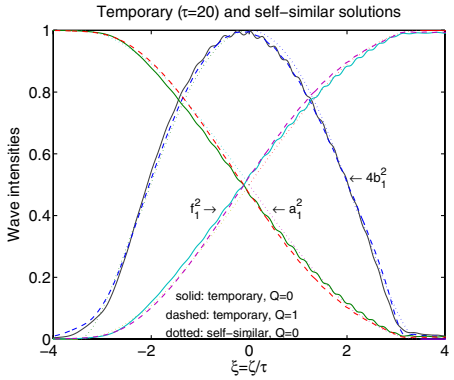

FIG. 2 (color online). The self-similar solution is an attractor, for $\tau \leq 20$, and it is not very sensitive to Q, for $|Q| \lesssim 1$.

relation between a_1 and f_1 follows therefrom, namely, the conservation law $a_1^2 + f_1^2 = \text{const} \approx 1$.

Further, the six unknown functions can be expressed in the terms of only two as follows:

$$a_1 = \cos(u/2), \qquad f_1 = \sin(u/2), \tag{6}$$

$$\alpha_\zeta \approx b_1 \tan(u/2), \qquad \phi_\zeta \approx b_1 \cot(u/2), \tag{7}$$

$$\beta_\zeta \approx \alpha_\zeta - \phi_\zeta \approx -2b_1 \cot u. \tag{8}$$

Substituting the above expressions into the complex Eq. (3) for $\tilde{b}$, one gets two real equations for the remaining two unknown functions,

$$(b_1^2)_\tau = 2(b_1^2\beta_\zeta)_\zeta - (\cos u)_\zeta/2, \tag{9}$$

$$\beta_\tau = \beta_\zeta^2 - (b_1)_{\zeta\zeta}/b_1 + \sin u/2b_1 + Qb_1^2. \tag{10}$$

The term $(b_1)_{\zeta\zeta}/b_1$, small in the WKB applicability range, can be neglected. Then, the equation set (8)–(10) gets a new symmetry that allows the self-similar substitution $\xi = \zeta/\tau$ and

$$b_1(\zeta,\tau) = G(\xi), \quad \beta(\zeta,\tau) = \tau B(\xi), \quad u(\zeta,\tau) = U(\xi), \tag{11}$$

leading to the following ordinary differential equations

$$G = -\tfrac{1}{2}B_\xi \tan U, \qquad \xi(G^2)_\xi = -2(G^2B_\xi)_\xi + \tfrac{1}{2}(\cos U)_\xi,$$
$$\cos U = B_\xi[\xi B_\xi - B + (B_\xi)^2 + QG^2]. \tag{12}$$

The ordinary differential equation (ODE) set (12), still complicated, can be dramatically simplified by the Legendre transformation $w = \xi\eta - B$, $\eta \equiv B_\xi$, which gives, for $\tilde{w} \equiv w + \eta^2$,

$$\cos U = \eta(\tilde{w} + QG^2), \qquad \sin U = -2G\cos U/\eta,$$
$$(\cos U)_\eta = 2[\tilde{w}_\eta (G^2)_\eta + 2G^2]. \tag{13}$$

When $w(\eta) = \tilde{w} - \eta^2$ is known, $B(\xi)$ is restored by the inverse Legendre transformation $\xi = w_\eta$, $B = \eta w_\eta - w$. Values of G and $\tilde{w}$ are linked by an algebraic equation,

$$(4G^2 + \eta^2)(\tilde{w} + QG^2)^2 = 1, \tag{14}$$

that can be used to reduce (13) to a single 1-order ODE for G as a function of the new independent variable η,

$$\left(\frac{dG}{d\eta}\right)^2 = \frac{(\eta^2 + 4G^2)^{3/2} - 1}{4 + Q(\eta^2 + 4G^2)^{3/2}}. \tag{15}$$

The physically relevant solution of this equation has maximum at $\eta = 0$ and looks at small η as

$$G = \frac{1}{2}\left[1 - \frac{\eta^2}{1 + \sqrt{(11 + 2Q)/3}} + O(\eta^4)\right]. \tag{16}$$

This solution, transformed back to the variable ξ, is presented in Fig. 2 by dotted line, for $Q = 0$. It is complemented by cases $Q = \pm 4$ in Fig. 3.

For larger τ, short wavelength modulations appear at the flattened top of the pumped pulse. The instability is analytically tractable, and it starts between $\tau = 20$ and $\tau = 25$, for $|Q| \lesssim 1$, as illustrated by Fig. 4. The allowed amplification distance z_M and the output pulse total duration Δt (corresponding to $\Delta\xi \approx 6$ in Fig. 2) can be determined from the formulas (4) for ζ and $\tau(\approx 20)$. Thus, by expressing c_b' in terms of Q, one has

$$z_M \approx \frac{20c_b}{a_0^{4/3}}\left[\frac{Qc_b}{(c_a + c_b)RV_3^2}\right]^{1/3}, \quad \Delta t \approx \frac{120}{a_0^{2/3}}\left[\frac{(c_a + c_b)R}{Qc_bV_3^4}\right]^{1/3}.$$

For BRA in plasmas, these formulas for z_M and Δt read

$$z_M \approx \frac{20(4|Q|)^{1/3}c}{a_0^{4/3}\omega_p}, \quad \Delta t \approx \frac{1.7[\lambda(\text{nm})]\text{fsec}}{|Q|^{1/3}(100a_0)^{2/3}}. \tag{17}$$

Note that the allowed amplification distance is larger in more rarefied plasmas, where ω_p is smaller. However, the plasma should be dense enough to avoid an excessive Langmuir wave breaking (which reduces coupling of the pump and pumped lasers). Near the wave-breaking limit, $\omega_p = \omega(4a_0)^{2/3}$, formula (17) for z_M turns into

$$z_M \approx 10(|Q|/4)^{1/3}\lambda/\pi a_0^2. \tag{18}$$

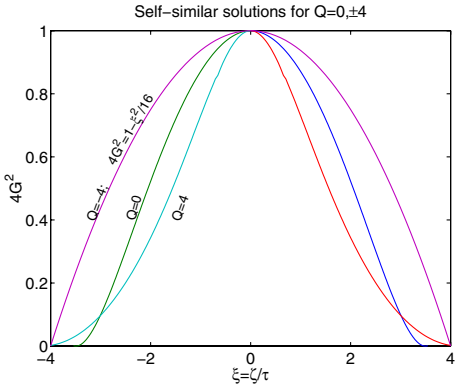

FIG. 3 (color online). Self-similar solution for several Q's. Note simple analytical formula for $Q = -4$.

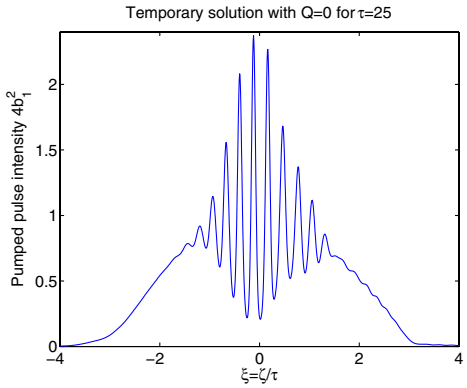

FIG. 4 (color online). Short wavelength instability develops at $\tau > 20$ when the pumped pulse top would become otherwise too flat.

Since the pump is completely depleted, the energy acquired by the pumped pulse within the distance z_M is equal to the energy of the $2z_M$-long pump pulse, i.e.,

$$E = 2\pi a_0^2 (m_e c^2/e\lambda)^2 z_M \approx 3.7|Q|^{1/3}\mathrm{J}/[\lambda(\mathrm{cm})]. \quad (19)$$

For $Q = 1$, this fluence exceeds by 10 times that in the uniform plasma. For $\lambda = 1$ nm, the fluence $E \approx 37$ MJ/cm^2 is acquired within the amplification distance $z_M \approx 2 \times 10^{-7} a_0^{-2}$ cm. For $a_0 = 0.03$, the amplification distance is 2 μm and the output pulse duration is 0.8 fs. This pulse could possibly be recompressed back to the 10 times shorter duration of 80 as. Note that for the efficient BRA, the seed-pulse front should be as short as the output pulse.

In summary, although inhomogeneities are generally thought to limit the resonant Raman amplification, it is shown how relic lattice effects can, in fact, be exploited to enhance Raman compression in the x-ray regime, opening up the possibility of generating attosecond x-ray pulses in plasmas produced by irradiation of crystalline solids. The analytical theory for the stimulated backscattering has been developed, taking into account the dispersion of group velocity and the nonlinear propagation of amplified pulses. For x-ray BRA in plasmas with relic crystal structure, the optimal value of the x-ray frequency band gap is found to be $\Delta \sim \omega_p^2/\omega$. At this value, the enhanced dispersion stabilizes the SPMI precisely upon reaching the greatest possible pulse compression in the π-pulse regime. The band gap can also suppress the generation of parasitic Stokes components of the amplified pulse. After completion of the π-pulse regime, the pulse can stretch and acquire the fluence 10 times larger than in the uniform plasma, before the new kind of instability, found above, develops. The stretched pulse can be recompressed back to the shortest duration by the complementary lattice, similar to the CPA technique, giving the potential to generate by this method x-ray pulses of 40 MJ/cm^2 fluences and 80 as durations.

This work was supported in part by the NNSA under the SSAA Program through DOE Research Grant No. DE-FG52-04NA00139. The authors thank E. Valeo for computational advice.

[1] R. Tatchyn *et al.*, Nucl. Instrum. Methods Phys. Res., Sect. A **375**, 274 (1996); www-ssrl.slac.stanford.edu/lcls.
[2] V. Ayvazyan *et al.*, Eur. Phys. J. D **37**, 297 (2006); SLAC Report No. SLAC-PUB-12114; DESY Deutsches Elektronen-Synchrotron Reports No. DESY 2002-167 and No. TESLA-FEL 2002-09, 2002; xfel.desy.de.
[3] C. J. Bocchetta *et al.*, Nucl. Instrum. Methods Phys. Res., Sect. A **507**, 484 (2003); www.elettra.trieste.it/FERMI.
[4] D. L. Smith *et al.*, IEEE Trans. Plasma Sci. **28**, 1316 (2000); www.llnl.gov/nif/project.
[5] M. Andre, Fusion Eng. Des. **44**, 43 (1999); www-lmj.cea.fr/html/cea.htm.
[6] P. Emma *et al.*, Phys. Rev. Lett. **92**, 074801 (2004); A. A. Zholents and W. M. Fawley, Phys. Rev. Lett. **92**, 224801 (2004); E. L. Saldin, E. A. Schneidmiller, and M. V. Yurkov, Opt. Commun. **212**, 377 (2002); **237**, 153 (2004); **239**, 161 (2004); A. A. Zholents, Phys. Rev. ST Accel. Beams **8**, 040701 (2005); A. A. Zholents and G. Penn, Phys. Rev. ST Accel. Beams **8**, 050704 (2005).
[7] V. M. Malkin, N. J. Fisch, and J. S. Wurtele, Phys. Rev. E **75**, 026404 (2007).
[8] B. J. Eggleton *et al.*, Phys. Rev. Lett. **76**, 1627 (1996); N. G. R. Broderick *et al.*, Phys. Rev. Lett. **79**, 4566 (1997); G. Lenz, B. J. Eggleton, and N. Litchinitser, J. Opt. Soc. Am. B **15**, 715 (1998).
[9] V. M. Malkin, G. Shvets, and N. J. Fisch, Phys. Rev. Lett. **82**, 4448 (1999).
[10] G. A. Mourou, C. P. J. Barty, and M. D. Perry, Phys. Today **51**, No. 1, 22 (1998); M. D. Perry, D. Pennington, and B. C. Stuart, Opt. Lett. **24**, 160 (1999).
[11] A. G. Litvak, Zh. Eksp. Teor. Fiz. **57**, 629 (1969) [Sov. Phys. JETP **30**, 344 (1970)]; C. Max, J. Arons, and A. B. Langdon, Phys. Rev. Lett. **33**, 209 (1974); G.-Z. Sun *et al.*, Phys. Fluids **30**, 526 (1987).
[12] D. L. Bobroff and H. A. Haus, J. Appl. Phys. **38**, 390 (1967).
[13] G. L. Lamb Jr., Phys. Lett. A **29**, 507 (1969); Rev. Mod. Phys. **43**, 99 (1971); *Elements of Soliton Theory* (Wiley, New York, 1980), Sec. 5.2, 7.8, 7.11; V. E. Zakharov, JETP Lett. **32**, 589 (1980); S. V. Manakov, JETP Lett. **35**, 237 (1982); V. A. Gorbunov, V. B. Ivanov, S. B. Papernyi, and V. R. Startsev, Izv. Akad. Nauk SSSR, Ser. Fiz. **48**, 1580 (1984); [Bull. Acad. Sci. USSR, Phys. Ser. **48**, 120 (1984)]; J. Coste and C. Montes, Phys. Rev. A **34**, 3940 (1986).
[14] A. Picozzi, C. Montes, and E. Picholle, Phys. Rev. E **58**, 2548 (1998).
[15] J. Crank and P. Nicholson, Proc. Cambridge Philos. Soc. **43**, 50 (1947); Adv. Comput. Math. **6**, 207 (1996).